COMPUTATIONAL INVESTIGATIONS OF POLYMER SHEET BREAKUP FOR OPTIMIZATION OF DEVOLATILIZATION PROCESSES IN STEAM CONTACTORS

BRAD SHINDLE[1] & ABHILASH J. CHANDY[2]
[1]Department of Mechanical Engineering, The University of Akron, USA
[2]Department of Mechanical Engineering, Indian Institute of Technology Bombay, Mumbai, India

ABSTRACT

Polymer devolatilization is a vital process in polymer manufacturing and is significantly impactful on the successful creation of high quality polymers, meeting both rigorous product specifications and regulatory requirements. One of the devolatilization methods that is the focus of this research is steam stripping, where superheated steam is used to remove any unwanted substances, such as volatiles and solvents, from the polymer mixture. This polymer mixture, referred to as "cement" and comprised of polymer and a volatile cyclohexane solvent, mixes with superheated steam and undergoes breakup into smaller droplets followed by phase change resulting in the removal of cyclohexane. The objective of the current study is embodied in two steps. The first step involves the development of a computational fluid dynamics (CFD)-based multiphase model that solves for the initial breakup of the liquid polymer mixture by steam. As part of this effort, detailed parametric studies are conducted to determine the effects of different contactor geometries on the initial sheet breakup, and the potential impact on the final polymer product quality. The second step then uses the resulting diameter distribution to model the multiphase heat and mass transfer of the polymer mixture including evaporation. Specifically, 3D CFD calculations are carried out using a Eulerian–Lagrangian approach, where the superheated steam is modelled as the continuous phase and tracked in a Eulerian frame, while the cement droplets are treated using a Lagrangian tracking method, thereby providing distributions of particle sizes, temperatures, and solvent content in the contactor. Results helped optimize the devolatilization process in terms of steam savings and volatile content in the final polymer.
Keywords: polymer devolatilization, CFD, multiphase.

1 INTRODUCTION

The quality of each polymer is paramount to the successful use of the material for its intended application, some of which range from agricultural and biomedical solutions to aerospace components and even to modern day clothing and accessories. High quality polymers, in particular, require significant refinement to meet product specifications and environmental regulations. Perhaps the most significant manufacturing process affecting quality is the process of polymer devolatilization. Essentially, polymer devolatilization is the removal of unwanted byproducts in the polymer mixture, such as monomers, solvents, and any other volatile products introduced when making the polymer [1].

The devolatilization process occurs inside a pressurized vessel called a steam contactor, to cause the polymer mixture to disintegrate into smaller liquid structures or droplets. These droplets continue to break apart as they are carried through the contactor by the superheated steam, which also serves as the heat source necessary to further evaporate the solvents. The resulting product mixture, comprised of a higher polymer content and a lower volatile content than at the start of the process, then undergoes additional processing to create granular polymer particles called "crumb".

The liquid polymer mixture in this research, hereon referred to as "cement", is comprised of polymer and cyclohexane, a hydrocarbon solvent. The superheated steam and cement are

WIT Transactions on Engineering Sciences, Vol 123, © 2019 WIT Press
www.witpress.com, ISSN 1743-3533 (on-line)
doi:10.2495/MPF190111

both injected into the annular space of the contactor via circumferential slits. The cement is injected downstream of the steam. The resulting interaction can be categorized into two different multiphase flow phenomenon: primary and secondary sheet breakup. The first occurs in the section of the contactor nearest the inlets as the cement comes into contact with the high pressure and temperature steam. Upon contact, the liquid column begins to shear apart into liquid ligaments and particles. The second phenomena occurs downstream as the droplets continue to experience heat transfer and aerodynamic forces from the steam, leading to further potential breakup and evaporation of the cyclohexane. The complexity and computational expense associated with modeling the multiphase flow interaction necessitates the development of a separate model for the secondary, multiphase flow regime.

Most polymers contain low-molecular weight components like unreacted monomers, solvents, and other by-products. These are collectively known as volatiles and are separated from the polymer for a variety of reasons, including regulatory requirements, polymer quality, and odor elimination [1]. This separation process is known as polymer devolatilization and can be accomplished utilizing either static or dynamic equipment, depending on the polymer mixture composition (e.g. volatile mass fraction) [2]. Static methods, as in this research, are particularly effective for the devolatilization of low-viscosity, high volatile mass fraction mixtures by causing the solvent to evaporate rapidly or flash [1], [3]. The flash occurs when the vapor pressure, p^*, of the volatile in the polymer mixture exceeds its own local partial pressure, p_v [4]. Because the vapor pressure is heavily dependent on temperature, the operating temperature of the polymer mixture must be high enough (without resulting in thermal degradation) to allow $p^* - p_v > 0$ upon injection into the static devolatilization equipment. The temperature increase is provided by a heated stripping agent like the superheated steam in this research. Despite being used for its simplicity and lower operating costs, the geometry and operating conditions of the static equipment must be optimized to prevent over- or under-exposure to the heated stripping agent and inconsistent final product quality [3].

Changes to the actual equipment and operating conditions in such manufacturing facilities would result in higher costs and loss of productivity, and hence, computational fluid dynamics (CFD) is a very cost-effective tool to evaluate a number of different modifications. Previous research by the same authors focused on developing a CFD model to simulate flow conditions in this problem [5, 6]. The model of this multiphysics process was used to optimize the consumption of costly superheated steam and evaluate the affects of geometry changes on droplet evaporation in the mixing and nanogap zones of the contactor [3], [7]. The objective of this paper is to further build on that research by assessing the impact of contactor design on the initial breakup of the polymer mixture near its inlet and on how much polymer mixture sticks to the walls of the vessel.

2 GEOMETRY

The steam contactor is a pressurized vessel where superheated steam and cement are mixed to accomplish the polymer devolatilization process. The dimensions of the steam contactor are shown in Fig. 1, which shows a cross-sectional view of the contactor, where the annular space is created by a plug (shown as hollow space in the figure) that fills the center of the contactor [3]. The total length of the contactor is 1320 mm with a maximum external diameter of 183 mm.

The process begins with the injection of superheated steam through a circumferential, annular slit at a 45° angle. Just downstream of the steam injection, cement is also injected into the annular space of the contactor through a circumferential slit. Injected normal to the contactor wall and into the incoming flow of steam, the cement is immediately affected by

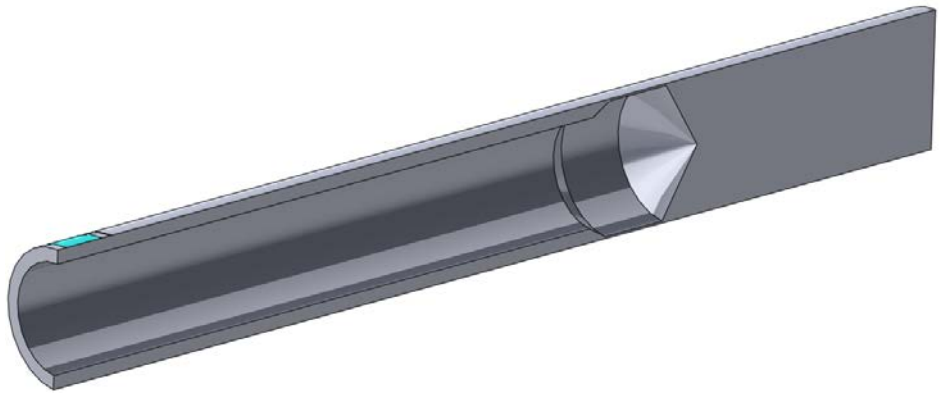

Figure 1: Cross-sectional view of entire G1 contactor.

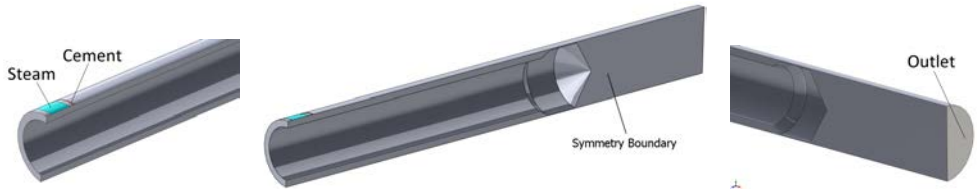

Figure 2: Geometry callouts for (left) steam and cement inlets, (center) symmetry boundary, and (right) outlet.

the momentum and temperature of the steam. Because the composition is 86% cyclohexane solvent and 14% polymer, the solvent begins to flash upon contact, starting the disintegration of the cement liquid column.

To balance computational efficiency and accuracy, primary breakup and the resulting multiphase flow after breakup are evaluated in two different models. Primary breakup is evaluated using a full three-dimensional model of the first 254 mm of the contactor. Secondary breakup is calculated via an axisymmetric 3D model of the entire contactor as shown in Fig. 2 [3]. The operating conditions (in bold) in Table 1 for the original G1 contactor based on current production settings. The boundary conditions were chosen based on prior research and results obtained through this study, which are described later in the thesis [3].

Table 1: Operating and boundary conditions of the contactor.

Parameter	Steam inlet	Cement inlet	Outlet
Boundary	Pressure inlet	Velocity inlet	Pressure outlet
Velocity	—	3.16 m/s	—
Pressure	2100 kPa	—	**140** kPa
Temperature	**599** K	**433** K	**366** K

The original contractor geometry is modified such that it includes an additional steam inlet slightly downstream of the current cement inlet. Depicted by Fig. 3, this inlet is intended to add additional heat to the flow and prevent the upstream steam inlet from *pressing* the cement onto the wall. Similar to the upstream steam inlet, the downstream inlet is a

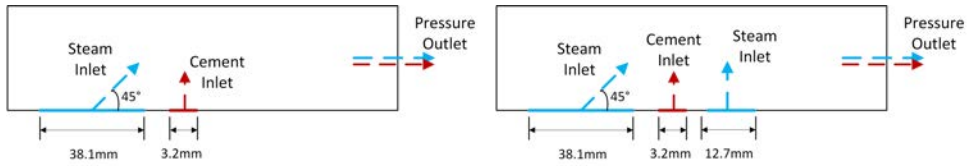

Figure 3: Plane schematic views of the bottom near the inlets for the original geometry (left) and the modified geometry (right).

circumferential, annular slit with the same operating and boundary conditions. Boundary conditions are altered in the modified geometry in order to maintain necessary production parameters, namely a cement mass flow rate of 3.9 kg/s and a steam-to-cement ratio of 0.6. These conditions were obtained as part of a separate optimisation effort related to cost savings with reducing the use of superheated steam [3].

This additional inlet is modeled in such a way that the steam is injected normal to the contactor walls.

3 FORMULATION

The governing equations in this study involve the Favre-averaged Navier–Stokes (FANS) equations given by

$$\frac{\partial \overline{\rho}}{\partial t} + \frac{\partial}{\partial x_i}\left(\overline{\rho}\tilde{u_i}\right) = 0, \tag{1}$$

$$\frac{\partial}{\partial t}\left(\overline{\rho}\tilde{u_i}\right) + \frac{\partial}{\partial x_i}\left(\overline{\rho}\tilde{u_j}\tilde{u_i}\right) = -\frac{\partial \overline{P}}{\partial x_i} + \frac{\partial}{\partial x_j}\left[\overline{t_{ji}} - \overline{\rho u_j'' u_i''}\right], \tag{2}$$

$$\begin{aligned}\frac{\partial}{\partial t}\left[\overline{\rho}\left(\overline{e} + \frac{\tilde{u_i}\tilde{u_i}}{2}\right) + \frac{\overline{\rho u_i'' u_i''}}{2}\right] + \frac{\partial}{\partial x_j}\left[\overline{\rho}\tilde{u_j}\left(\tilde{h} + \frac{\tilde{u_i}\tilde{u_i}}{2}\right) + \tilde{u_j}\frac{\overline{\rho u_i'' u_i''}}{2}\right] \\ = \frac{\partial}{\partial x_j}\left[-q_{L_j} - \overline{\rho u_j'' h''} + \overline{t_{ji}u_i''} - \overline{\rho u_j'' \tfrac{1}{2} u_i'' u_i''}\right] + \frac{\partial}{\partial x_j}\left[\tilde{u_i}\left(\overline{t_{ij}} - \overline{\rho u_i'' u_i''}\right)\right],\end{aligned} \tag{3}$$

and also the ideal gas equation given by

$$P = \overline{\rho} R \tilde{T}. \tag{4}$$

In eqns (1), (2), and (3), $(\ldots)''$ represents the fluctuating quantity [8], [9]. ρ is the density, u is the velocity, P is the pressure, t_{ji} is the viscous stress tensor, e and h are the specific internal energy and specific enthalpy, respectively, and q_{L_j} is the laminar mean heat flux. Eqn (4) is the Favre-averaged ideal gas equation used to model the continuous steam phase. In this problem, the Ma attained inside of the contactor is above 1, which makes the flow compressible, and hence modeling the steam as an ideal gas is apropos. The viscous stress tensor is written as: Turbulence modeling is achieved ion the simulations here through the RNG $k-\epsilon$ model. This model has shown to demonstrate improved accuracy for capturing the effect of swirl on turbulence and hence is appropriate for this simulation [10]–[13]. In addition, a species transport model is used to solve for the steam and cyclohexane vapor species using a convection-diffusion equation [13].

3.1 Volume of fluid interface tracking method for primary breakup

To perform a simulation showing the primary breakup of the cement injection within the G1 contactor, a separate model is used. In this model, the continuous steam phase is already in motion flowing through the contactor's main body, and the cement is added in as a liquid. As the liquid enters the contactor, it is quickly sheared apart into droplets. Since the interface between the gas and cement phase is not dispersed, an optimized version of the Volume of Fluid (VOF) interface tracking method, called the Coupled Level Set VOF (CLSVOF) [14] is employed here. This method combines the Level-Set (LS) method, first introduced by Li et al. [15], and the VOF tracking method. The volume fraction equation tracks the interface between the gas and liquid phases. A solution is found by solving the continuity equation for the volume fraction of one of the phases. For the ith phase, the continuity equation to solve the volume fraction is given as

$$\frac{1}{\rho_i}\left[\frac{\partial}{\partial t}\left(\alpha_i\rho_i\right) + \nabla\cdot\left(\alpha_i\rho_i\vec{v}_u\right) = \sum_{p=1}^{n}\left(\dot{m}_{pi} - \dot{m}_{ip}\right)\right]. \tag{5}$$

Here, the term α_i represents volume fraction of the ith fluid within the cell, thus α_i is zero when the cell is empty of the ith, 1 when the cell is completely full of the ith fluid, and between 0 and 1 when the cell contains and interface between the ith fluid and the other fluid. Additionally, $\dot{m}_{ip}$ is the mass transfer from phase i to phase p and $\dot{m}_{pi}$ is the mass transfer from phase p to phase q. More details can be found in [16].

3.2 Discrete phase model for secondary phase change

To predict the trajectory of the discrete phase particles in the secondary phase change step of the model, a discrete phase model (DPM) formulation is used, which integrates the force balance on the particle in a Lagrangian reference frame. This force balance equates the particle inertia with the forces acting on the particle, and can be written as

$$\frac{du_p}{dt} = F_D(\vec{u} - \vec{u}_p) + \frac{\vec{g}(\rho_p - \rho)}{\rho_p}, \tag{6}$$

where $F_D(\vec{u} - \vec{u}_p)$ is the drag force per unit particle mass, given by

$$F_D = \frac{18\mu}{\rho_p d_p^2}\frac{C_D Re}{24}, \tag{7}$$

and $\vec{u}$ is the continuous phase velocity, $\vec{u}_p$ is the particle velocity, μ is the dynamic viscosity of the fluid, ρ is the density, ρ_p is the density of the particle, and d_p is the particle diameter. Also, a high-Mach number drag law is also used here to account for the high-speed flows. In the context of the DPM, a convection/diffusion controlled vaporization model is used. In addition, boiling rate and energy equations are solved as well. Using the velocity fluctuations caused by turbulence, the particle trajectories are tracked as the particles flow through the domain, through the use of the stochastic discrete random walk (DRW) model is used [17]. To account for the coupling between the gas and particle phase, momentum exchange, heat exchange, and mass exchange are all calculated within the simulation.

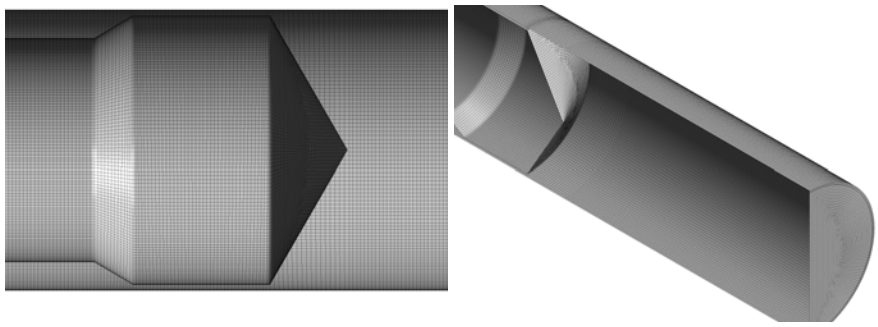

Figure 4: 3D axisymmetric contactor view of (top) mixing zone and gap region near the end of the contactor (bottom) outlet and divergence region.

4 COMPUTATIONAL DETAILS

4.1 Mesh

The simulations to measure primary breakup are set up using a CLSVOF model in ANSYS Fluent for a shorter 254 mm section of the full 3D contactor. The stable droplet diameter for this problem is calculated to be 143 μm, which requires that the maximum grid size to be equal to that value. As a result, a hexahedral-dominant mesh is employed here, which consists of approximately 3×10^6 grid points. On the other hand, for the secondary phase change, the entire contactor length is used to evaluate and track particle locations. Similar to the mesh for primary breakup, a hexahedral dominant mesh is used to improve accuracy and convergence. For this research, a mesh size of approximately 725,000 elements and 795,000 nodes is used and is shown in Fig. 4. Earlier research shows, through mesh dependence tests, that this mesh size is sufficient to accurately capture the parameters of interest [3], [6], [7].

4.2 Numerical methods

The CLSVOF model is a transient simulation that simultaneously solves for both the continuous and discrete phases (steam and cement, respectively). Listed below are the schemes used to solve the model based on research and ANSYS guidance [13], [18], [19].

- Pressure-Velocity Coupling: SIMPLE
- Pressure: PRESTO! (PREssure STaggering Option)
- Momentum, Density, Energy, Turbulence: First Order Upwind
- Gradient: Least Squares Cell Based
- Level-set Function: First Order Upwind
- Time: First Order Upwind Implicit
- Volume Fraction: Geo-Reconstruct

The Geo-Reconstruct scheme is particularly useful for time-dependent solutions with sharp interface between phases like those in this research.

The DPM simulation benefits from the accuracy of a second-order upwind discretization. A maximum number of trajectory time steps is set to 42,000 with a default step length factor of 5. The time step necessary to progress the DPM injections and solve for particle trajectories is chosen to be 0.0001 s. The choice of the current parameters is based on several numerical tests carried out previously [3]. All boundaries in the model are set as reflective, except for

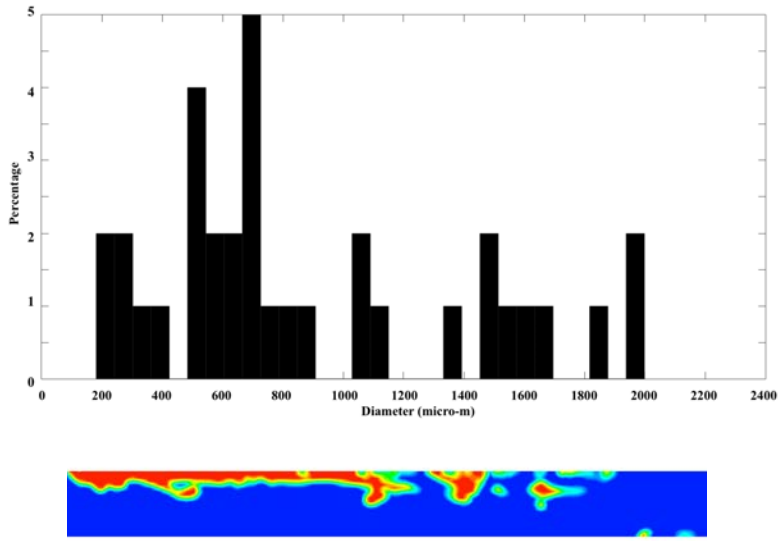

Figure 5: Upper plane view of original geometry CLSVOF results and associated particle diameter distribution from image analysis.

the outlet. For the purposes of this simulation, the particle interaction with the walls of the contactor is assumed to be completely elastic, meaning the particle retains all of its normal and tangential momentum after the collision [13]. The outlet is set to an escape boundary condition so that it is the only exit for the particles from the contactor, except in cases of reverse flow at the inlets.

5 RESULTS AND DISCUSSIONS

5.1 Primary breakup

The simulations to determine primary breakup are set up using a CLSVOF model in ANSYS Fluent for a shorter 254 mm section of the full 3D contactor. This length has been determined to be sufficient for viewing the initial liquid atomization from previous studies, which included validation with experiments as well [3]. The intent is to capture just the initial droplet formation without going through the computational expense of seeing further phase change, which will be modeled in a separate 3D axisymmetric DPM model.

So once the inlet and outlet flow conditions reach a relative equilibrium and uniformity, images of the breakup were analysed in an image analysis formulation in MATLAB. The diameter distributions are plotted in the form of a histogram form, anything above 3000 μm is neglected as being either a part of the initial liquid stream or captured against the wall without separation, leaving the total histogram percentage less than 100%. Because of this limitation, little consideration is afforded towards the amount of cement sticking to the wall and its impacts on the final polymer crumb quality. A comparison of the minimum, maximum, and average diameters resulting from the CLSVOF results for each geometry is provided in Table 2. The original geometry's distribution, visually depicted in Fig. 5, appears "favorable" (towards a better quality polymer crumb) with a majority of particles being less than 1000

Table 2: Minimum, average, and maximum droplet diameter in μm for each geometry.

Geometry	Min	Avg	Max
Original	181	944	1998
Modified	127	1662	1941

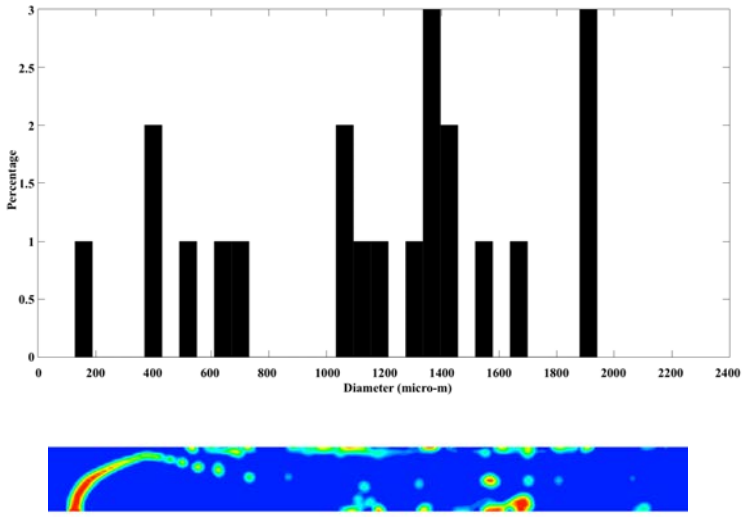

Figure 6: Lower plane view of Dual Steam – 90° CLSVOF results and associated particle diameter distribution from image analysis.

μm in diameter. It also has some of the smallest droplets created, which are only at 181 μm in diameter. This, in large part, is due to separation that occurs as the cement droplets "shed" from the column of fluid moving along the wall. This primary breakup is different than in any of the other geometries considered and reflects more of a bag-type breakup described earlier.

In the modified geometry, the downstream steam inlet injects superheated steam normal to the wall of the contactor. This downstream steam inlet forces the column of cement liquid to become more vertical, which leads to a reduced flowrate of steam coming from the upstream inlet as it comes into contact with the dense cement mixture. This interaction between the two steam flows leads to higher aerodynamic forces, shearing the cement unevenly and nearer to the opposite wall. This can be observed in the image and histogram shown in Fig. 6.

5.2 Secondary phase change

The second stage of the simulation effort involves the DPM calculations in ANSYS Fluent. In these calculations the entire contactor length is considered in order to evaluate relevant parameters of the outlet particles prior to entering the coagulation process. The transition from the CLSVOF model to the DPM model is accomplished by determining the particle diameters from the CLSVOF calculations, fitting them to a Rosin-Rammler distribution, and then employing them as inlet conditions for the particle injections in the DPM calculations. When the number of particles exiting equal the number being injected and when the flow is

Table 3: Comparison of outlet particle parameters.

	Diam (μm)	Res Time (s)	Cyclohexane MF	Temp (K)
Original (Min)	84.7	0.021	0.000	283.7
Dual steam (Min)	59.9	0.019	0.000	271.9
Original (Avg)	727.8	0.046	0.537	322.2
Dual steam (Avg)	699.8	0.031	0.484	321.5
Original (Max)	1687.4	0.069	0.815	474.7
Dual steam (Max)	1589.3	0.038	0.768	493.7

considered to be reasonably uniform, and at this stage, a sample of the particles at the outlet is picked in order to determine diameter, cyclohexane mass fraction, residence time, and temperature. The comparison of those results is shown in Table 3. The results of the original geometry have been validated with experimental data measured in the manufacturing facility of the industrial partner. From this table and from the corresponding histogram plots of the same parameters in Fig. 7, a couple of observations can be made. Firstly, while the effects on the minimum and maximum diameters are relatively equal between the models, the average particle diameter in the dual steam geometry is reduced by 30% more than in the original geometry. Secondly, an interesting feature of the results that seems counter-intuitive to the first observation is that the maximum particle residence time is 45% lower than in the original geometry. It is possible that one could erroneously assume that the average and maximum particle diameters would be larger due to the lesser residence time in the contactor and therefore lesser solvent evaporation. As mentioned previously, the results clearly show lower minimum, maximum, and average particle diameters than those from the original geometry calculation. Also, as it relates to the cyclohexane mass fraction, Fig. 8 show that the content is noticeably lower before the converging-diverging region of the contactor due to elevated particle temperatures.

The reason for this behaviour lies in the particle velocity predictions shown in Fig. 9. It can be seen here that at the outer edges of the original contactor, there are exceedingly slow moving particles (indicated by the dark blue-colored particles) depicting very high levels of cyclohexane mass fraction (as seen in Fig. 8) and also exceedingly low values of temperature (not shown here). This is increasingly true at the bottom of the contactor where it is likely that large stagnate particles have settled to the bottom of the contactor due to gravity. This is further supported by the residence time predictions (not shown here), where the particles with the longest residence time are coming from the bottom of the contactor. These particles would represent larger, stagnate cement adhering to the wall.

In the dual steam design, this occurs to a much lesser extent, because the figures depict a more uniform set of properties. This is a result of mixing with the superheated steam. Where there is insufficient contact with the steam, as in the case of geometries like the original contactor where much of the cement is adhering to the wall, then there is poor solvent removal regardless of residence time. When the amount of cement sticking to the wall is reduced, cyclohexane removal is enhanced, and the particles flow through the contactor as intended.

6 CONCLUSIONS

The intent of this research is to accurately model the polymer devolatilization process and the effects of contactor design changes on the final polymer product quality. Because of the complexity of the devolatilization process, measurements in the production facility are cumbersome and expensive. Therefore, the use of CFD modeling is particularly effective at

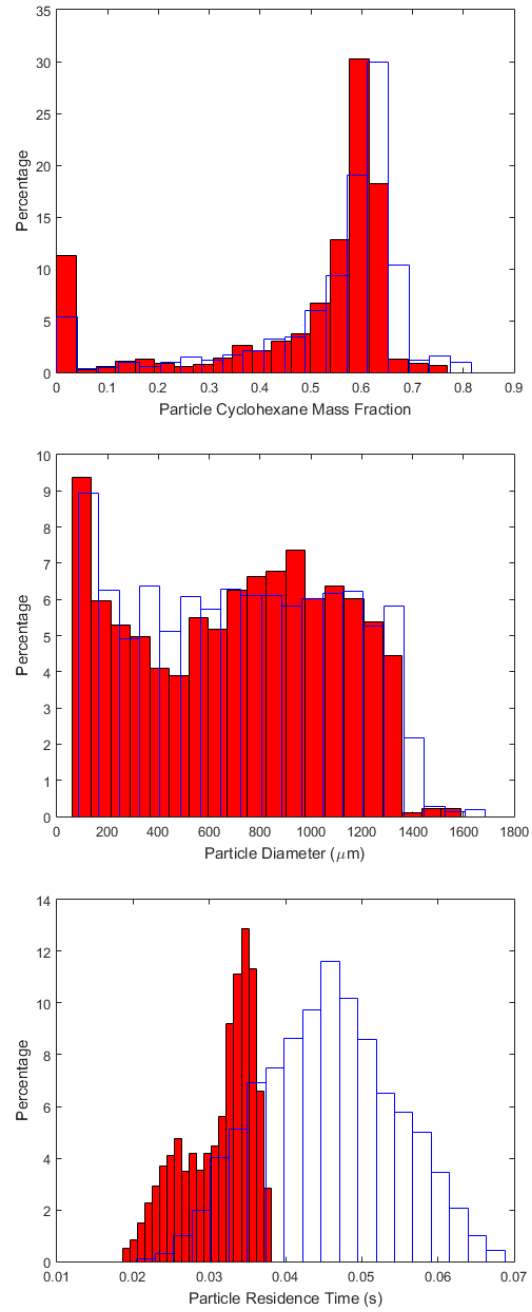

Figure 7: Histograms of cyclohexane mass fraction (top), diameter (middle) and residence time (bottom) of the particles at the outlet; open bars – original geometry, closed bars – modified geometry.

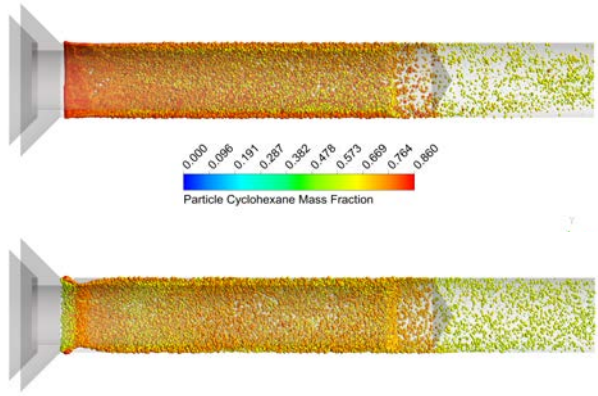

Figure 8: Particle cyclohexane mass fraction tracks for (top) original geometry and (bottom) dual steam inlets – 90°.

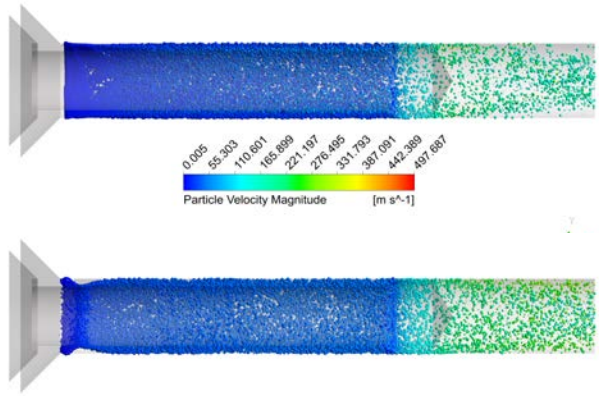

Figure 9: Particle velocity magnitude tracks for (top) original Geometry and (bottom) dual steam inlets – 90°.

providing a high confidence, lower cost solution. Towards this effort, 3D CFD calculations of polymer devolatilization in a steam contactor are conducted in two stages. The first stage develops a multiphase model for the initial or primary breakup of the liquid polymer mixture by steam. This stage employs the CLSVOF-based multiphase model to analyse the droplet diameter distribution in two different designs, where a polymer mixture sheet is stripped into droplets by superheated steam. The second stage then uses the resulting diameter distribution to model the secondary phase change of the polymer mixture. In this stage, the Eulerian–Lagrangian DPM approach is employed to model the phase change involving evaporation of polymer mixture droplets into polymer crumb. Results showed that slight geometric modifications resulted in ideal droplet diameter distributions and furthermore in increasing heat transfer and cyclohexane evaporation in the body the contactor at the stage of phase change.

REFERENCES

[1] Albalak, R., *Polymer Devolatilization*, Vol. 33, CRC Press, 1996.
[2] Tadmor, Z. & Gogos, C.G., *Principles of Polymer Processing*, John Wiley & Sons, 2013.
[3] Gabor, K.M., *Computational investigations of polymer devolatilization processes in steam contactors*. PhD thesis, The University of Akron, 2016.
[4] Astarita, G. & Maffettone, P.L., Devolatilization of polymers. *Adv. Transport Proc.*, **9**, 1993.
[5] Shindle, B., Gabor, K.M. & Chandy, A.J., Modeling polymer sheet breakup for devolatilization processes in steam contactors. *2nd Thermal and Fluids Engineering Conference (TFEC)*, ASTFE: Las Vegas, NV, USA, Paper # 18457, 2017.
[6] Gabor, K.M., Shindle, B. & Chandy, A.J., CFD investigation of control parameters of a steam contactor used in polymer devolatilization. *International Journal of Thermal Sciences*, **120**, pp. 19–30, 2017.
[7] Gabor, K.M., Shindle, B. & Chandy, A.J., CFD simulations of polymer devolatilization in steam contactors. *Engineering Applications of Computational Fluid Mechanics*, **11**(1), pp. 273–292, 2017.
[8] Walters, D.K. & Cokljat, D., A three-equation eddy-viscosity model for Reynolds-averaged Navier-Stokes simulations of transitional flow. *Journal of Fluids Engineering*, **130**, pp. 1–14, 2008.
[9] Burns, A.D., Frank, T., Hamill, I. & Shi, J.M., The Favre averaged drag model for turbulent dispersion in Eulerian multi-phase flows. *International Conference on Liquid Atomization and Spray Systems*, 2006.
[10] Papageorgakis, G. & Assanis, D.N., Comparison of linear and nonlinear RNG-based k-epsilon models for incompressible turbulent flows. *Numerical Heat Transfer: Part B: Fundamentals*, **35**(1), pp. 1–22, 1999.
[11] Hou, Q. & Zou, Z., Comparison between standard and renormalization group k-epsilon. models in numerical simulation of swirling flow tundish. *ISIJ International*, **45**(3), pp. 325–330, 2005.
[12] Jawarneh, A.M., Tlilan, H., Al-Shyyab, A. & Ababneh, A., Strongly swirling flows in a cylindrical separator. *Minerals Engineering*, **21**(5), pp. 366–372, 2008.
[13] ANSYS Academic Research, Help System, *ANSYS FLUENT Theory Guide*. Release 14.5 edition, 2012.
[14] Sussman, M. & Puckett, E.G., A coupled level set and volume-of-fluid method for computing 3d and axisymmetric incompressible two-phase flows. *Journal of Computational Physics*, **162**(2), pp. 301–337, 2000.
[15] Li, X., Massarotti, N., Nithiarasu, P., Ray, B., Biswas, G., Sharma, A. & Welch, S.W., CLSVOF method to study consecutive drop impact on liquid pool. *International Journal of Numerical Methods for Heat & Fluid Flow*, **23**(1), pp. 143–158, 2013.
[16] Shindle, B.W., *Computational investigations of polymer sheet breakup For optimization of devolatilization processes in steam Contactors*. PhD thesis, The University of Akron, 2017.
[17] Ajilkumar, A., Sundararajan, T. & Shet, U., Numerical modeling of a steam-assisted turbular coal gasifier. *International Journal of Thermal Sciences*, **48**, pp. 308–321, 2008.
[18] Andreassi, L., Baudille, R. & Biancolini, M.E., Spew formation in a single lap joint. *International Journal of Adhesion and Adhesives*, **27**(6), pp. 458–468, 2007.
[19] Cloete, S.W., Eksteen, J.J. & Bradshaw, S.M., A mathematical modelling study of fluid flow and mixing in full-scale gas-stirred ladles. *Progress in Computational Fluid Dynamics, An International Journal*, **9**(6-7), pp. 345–356, 2009.